

Tunable Cobalt Vacancies and Related Properties in LaCo_xAs_2

Shijie Shen,[†] Gang Wang,^{*,†} Shifeng Jin,[†] Qingzhen Huang,[‡] Tianping Ying,[†] Dandan Li,[†] Xiaofang Lai,[†] Tingting Zhou,[†] Han Zhang,[†] Zhiping Lin,[†] Xiaozhi Wu,[†] and Xiaolong Chen^{*,†,§}

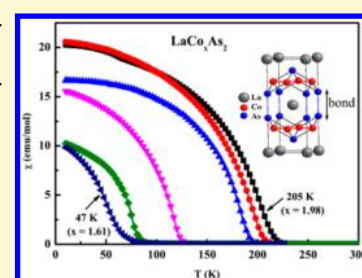
[†]Research & Development Center for Functional Crystals, Beijing National Laboratory for Condensed Matter Physics, Institute of Physics, Chinese Academy of Sciences, Beijing 100190, China

[‡]NIST Center for Neutron Research, NIST, Gaithersburg, Maryland 20899-6102, United States

[§]Collaborative Innovation Center of Quantum Matter, Beijing 100084, China

Supporting Information

ABSTRACT: The origin of transition metal vacancies and their effects on the properties of ThCr_2Si_2 -type compounds have been less studied and poorly understood. Here we carefully investigate the structure, physical properties, and electronic structure for a series of lanthanum cobalt arsenides with nominal composition of LaCo_xAs_2 ($1.6 \leq x \leq 2.1$). It is revealed that the occupancy of Co can be tuned between 1.98(1) and 1.61(1). The structural analyses based on X-ray and neutron diffractions show the existence of Co vacancies results from charge balance due to the formation of bond between As–As. These Co vacancies affect the magnetic and electrical properties greatly, adjusting the Curie temperature from 205 to 47 K and increasing the resistivity by more than 100%. First-principles calculations indicate that the Co vacancies weaken the spin polarization and reduce the density of states at the Fermi level, resulting in decreased Curie temperature and increased resistivity, respectively. Our results address the importance of transition metal vacancies in ThCr_2Si_2 -type materials and offer a reliable route to tune the magnetism of ThCr_2Si_2 -type structure.



INTRODUCTION

The ThCr_2Si_2 -type structure, composed of covalently bonded transition metal–metalloid layers and the intermediate metals, which are usually alkalis, alkali earths, and lanthanides, is a common structure to around 1000 compounds.¹ Among them, 3d transition metal-contained compounds account for the majority. These compounds exhibit rich physical properties, such as the heavy Fermion behavior,^{2,3} the reentrant ferromagnetism,⁴ the ferromagnetic quantum critical transition,⁵ and superconductivity as well.^{6–9} It is believed that the electron transfer from the intermediate metals to the layers and the valent state of 3d metals play important roles in determining the properties.

The electron transfer and the valent state of the 3d metal are highly correlated. If the amount of electron transfer exceeds what the layers can accommodate, with a 3d metal adopting its lowest stable valence, vacancies in the layers are expected. In this context, the formation of bonds between interlayer metalloids can also contribute to the occurrence of 3d metal vacancies in the layers. This is particular true for the late 3d metal-contained ThCr_2Si_2 -type compounds. For instance, Ni, Cu, and Co vacancies are often observed in their corresponding compounds.^{10–13} But the vacancies of Ni and Cu have no effect on the magnetism for Ni and Cu carry no localized magnetic moment. In contrast, the vacancies of Co can influence the magnetic property to some extent and have attracted interests. It has been reported that the existence of a little bit of Co vacancies lowers the Neel temperature from about 70 to 52 K

for CaCo_2As_2 .¹³ Recent studies showed that Co vacancies exist in compounds RCO_2As_2 ($R = \text{La, Ce, Pr, Nd}$).^{14,15}

Thompson et al.¹⁴ demonstrated that LaCo_2As_2 undergoes a ferromagnetic transition at 86 K and highlighted the significant enhancement of T_c (above 200 K), which is attributed to unintentional incorporation of a small amount of Bi and the formation of vacancies in the Co sublattice. The effect of incorporated Bi into the structure is emphasized.¹⁴ However, it is not easy to understand that such a small amount of Bi (3.1%) could induce a significant increase in T_c . Here, we report a careful investigation of crystal structure, physical properties, and electronic structure of LaCo_xAs_2 as a function of Co occupancy for nominal $1.6 \leq x \leq 2.1$. It is revealed that Co vacancies up to 19% can exist in collapsed tetragonal (cT) LaCo_xAs_2 due to the formation of As–As bonding. We find that these Co vacancies in turn strengthen the As–As bonding, increase the resistivity, and most importantly, alter the temperature of magnetic ordering from 205 to 47 K. The results show the possibility of tuning the magnetization of ThCr_2Si_2 -type structure by transition metal vacancies.

EXPERIMENTAL SECTION

Starting Materials. Powder of As (Aladdin, 99.995%) was used as received. Finely dispersed chipping of La (Alfa Aesar, 99.9%) was used after carefully scraping away the surface layer. Co powder (Alfa Aesar,

Received: August 12, 2014

Revised: October 16, 2014

Published: October 21, 2014

99.8%) was additionally purified by heating under a flow of NH_3 gas at $500\text{ }^\circ\text{C}$ for 30 min.

Synthesis. The starting materials were mixed in ratios of La:Co:As = 1.0: x :2.0 ($x = 2.1, 2.0, 1.9, 1.8, 1.7,$ and 1.6 , total mass is about 1.5 g). Then they were pelletized and loaded in alumina crucibles. The crucibles were sealed inside silica tubes, which were backfilled with about 0.3 atm high purity argon gas. The samples were heated to $610\text{ }^\circ\text{C}$ with a constant heating rate ($100\text{ }^\circ\text{C/h}$), held there for 12 h (prereacting the volatile As with Co), then to $850\text{ }^\circ\text{C}$ for 24 h (reacting the La chipping with As and Co to obtain a precursor for the second cycle). After carefully grinding, the samples were then heated at $1100\text{ }^\circ\text{C}$ for 48 h and furnace-cooled to room temperature. All manipulations for sample preparation were carried out inside an argon-filled glovebox (content of $\text{O}_2 < 1$ ppm).

X-ray and Neutron Diffraction. Room temperature powder X-ray diffraction (PXRD) data of nominal LaCo_xAs_2 ($x = 2.1, 2.0, 1.9, 1.8, 1.7,$ and 1.6) were collected using a PANalytical X'pert Pro diffractometer with $\text{Co K}\alpha$ radiation (40 kV, 40 mA) and a graphite monochromator in a reflection mode ($2\theta = 10^\circ$ to 130° , step = 0.017° (2θ), and scan speed = 0.4 s/step). Neutron powder diffraction of nominal $\text{LaCo}_{1.8}\text{As}_2$ was performed ($T = 300\text{ K}$) at BT1 neutron powder diffractometer at NIST Center. A Cu (311) monochromator was used to produce the monochromatic neutron beam with the wavelength $\lambda = 1.5398\text{ \AA}$. Collimations of $60', 15',$ and $7'$ were used before and after monochromator and after sample, respectively. Neutron powder diffraction of nominal $\text{LaCo}_{2.0}\text{As}_2$ was performed ($T = 220$ and 4 K) with a Ge (733) monochromator with the wavelength $\lambda = 1.1969\text{ \AA}$. Rietveld refinements of the data were performed with the FULLPROF package.¹⁶ The structure of ThCr_2Si_2 was used as starting model for refinements of all these compounds. Only the z fraction coordinate of As atom is refinable among all atomic coordinates due to the restraint of the symmetry. During the refinements, a strong correlation between temperature factors and occupancy factors was observed, trying to refine the structures without restraint of temperature factors will lead to unreasonable results. So the temperature factors of La, Co, and As atoms were restrained to the values obtained from a single-crystal X-ray diffraction of $\text{La}_{0.97(1)}\text{Bi}_{0.03(1)}\text{Co}_{1.91(1)}\text{As}_2$ ¹⁵ for all the refinements.

Energy-Dispersive X-ray Spectroscopy (EDX). The Co content of nominal LaCo_xAs_2 ($x = 2.1, 2.0, 1.9, 1.8, 1.7,$ and 1.6) samples was characterized by EDX. The result for each sample was obtained based on the average of three sets of data.

Physical Property Measurements. The static (DC) magnetic susceptibility of nominal LaCo_xAs_2 ($x = 2.1, 2.0, 1.9, 1.8, 1.7,$ and 1.6) was measured using a vibrating sample magnetometer (Quantum Design) in an applied field of 100 Oe at the temperatures ranging from 10 to 300 K. Temperature-dependent electrical resistivity measurements for nominal LaCo_xAs_2 ($x = 1.6$ and 2.1), which were cold-pressed under a uniaxial stress of 400 kg cm^{-2} , were performed using the standard four-probe method on the physical property measurement system (Quantum Design) at the temperatures between 10 and 300 K.

Electronic Structure Calculations. Band structure calculations were performed using the CASTEP program code with plane-wave pseudopotential method.¹⁷ We adopted the generalized gradient approximation with Perdew–Burke–Ernzerhof formula for the exchange–correlation potentials.¹⁸ The ultrasoft pseudopotential with a plane-wave cutoff energy 330 eV and a Monkhorst Pack k -point separation of 0.04 \AA^{-1} in the reciprocal space were used for the calculations.¹⁹ The self-consistent field was set as $5 \times 10^{-7}\text{ eV/atom}$.

Full structural optimization including the lattice parameters and the atomic positions was performed with the convergence standard given as follows: energy change less than $5 \times 10^{-6}\text{ eV/atom}$, residual force less than 0.01 eV/\AA , stress less than 0.02 GPa, and displacement of atom less than $5 \times 10^{-4}\text{ \AA}$. Calculations were performed on two compounds, one is LaCo_2As_2 with complete CoAs layers, the other $\text{LaCo}_{1.5}\text{As}_2$ with ordered Co vacancies. Supercells $\sqrt{2} \times \sqrt{2} \times 1$ were built accordingly with two CoAs layers having total of eight Co/vacancy sites. Calculations on the magnetic order were performed assuming ferromagnetic ordering of all Co atoms within the structure.

RESULTS AND DISCUSSION

Figure 1 displays the PXRD patterns using $\text{Co K}\alpha$ radiation for a series of LaCo_xAs_2 samples with nominal x of 2.1, 2.0, 1.9, 1.8,

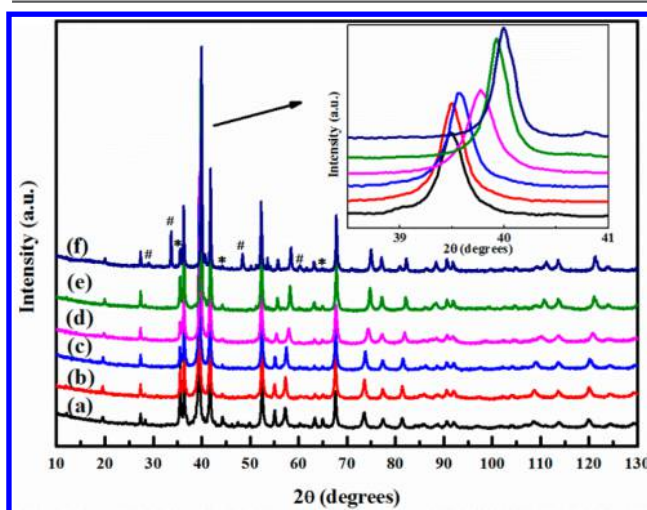


Figure 1. PXRD patterns of nominal LaCo_xAs_2 ($x = 2.1, 2.0, 1.9, 1.8, 1.7,$ and 1.6 in (a)–(f), respectively) $\text{Co K}\alpha$ radiation. The reflections marked by (*) and (#) are assigned to LaOCeAs and LaAs , respectively. The inset shows the enlarged (103) peak.

1.7, and 1.6 collected at room temperature. The main phase can be well indexed on the body-centered tetragonal cell (space group $I4/mmm$). The side phase (marked by asterisk) is assigned to LaOCeAs , which is hard to be eliminated by various attempts. It is also noticed that side phase LaAs arises at nominal $x = 1.6$. As shown from the inset of Figure 1, the strongest peak of the main phase shifts gradually to higher angle with the decreasing nominal content of Co from 2.1 to 1.6. It manifests that the structure has a significant homogeneity range with respect to Co.

Figure 2 shows the Rietveld refinements for PXRD data of nominal $\text{LaCo}_{1.8}\text{As}_2$. The final agreement factors converge to $R_p = 2.45\%$, $R_{wp} = 3.20\%$, and $R_{exp} = 1.50\%$. Refinements of the site occupation factors result in significant deviation from unity

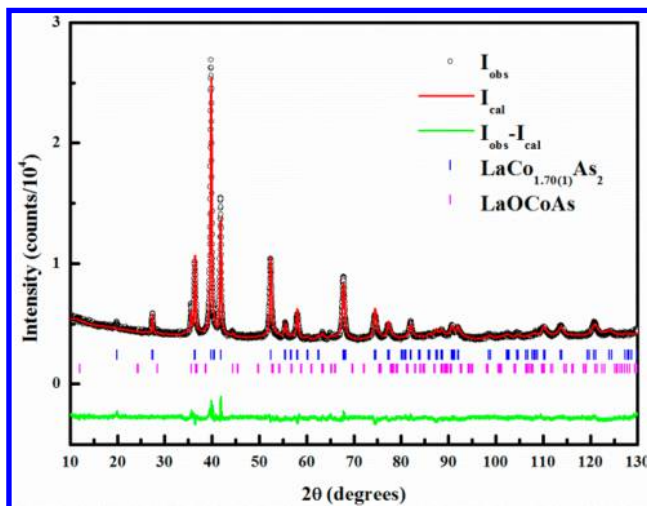


Figure 2. PXRD pattern of nominal $\text{LaCo}_{1.8}\text{As}_2$. The Rietveld refinement fits, difference profiles, and positions of Bragg peaks are also shown.

for Co, but the La and As sites are fully occupied. The refined Co occupancy is 1.70(1). To explore the possibility of Co/As mix-occupancy, we did a concurrent refinement which takes into account the Co/As mix-occupancy on the Co-site and As-site and obtained both negative values, which manifest that Co/As mix-occupancy is unlikely in the compounds. Neutron diffraction (Supporting Information Figure S1a) confirms the existence of Co vacancies. The refined Co content of nominal $\text{LaCo}_{1.8}\text{As}_2$ is 1.72(3), which is consistent with the PXRD data.

Rietveld refinements for other nominal LaCo_xAs_2 ($x = 2.1, 2.0, 1.9, 1.7,$ and 1.6) against PXRD data were also performed (Supporting Information Figure S2). All the crystallographic data including the molar ratios of phases are summarized in Supporting Information Table S1. What deserves to be mentioned is that the deficiency of Co is an intrinsic feature for LaCo_xAs_2 , the actual Co content is tunable between 1.98(1) and 1.61(1), with maximum vacancy ratio up to 19% ($x = 1.61$). EDX measurements were conducted to confirm the trend in variation of Co content across the series of samples. As shown in Table 1, the variation trend of Co content is in

Table 1. Comparison of Nominal, Refined and EDX Characterized Co Content for Nominal $\text{LaCo}_x\text{As}_2^a$ Samples^b

nominal	refined	EDX
2.1	1.98(1)	1.8(1)
2.0	1.92(1)	1.7(1)
1.9	1.82(1)	1.7(1)
1.8	1.70(1)	1.6(1)
1.7	1.64(1)	1.6(1)
1.6	1.61(1)	1.5(1)

^a $x = 2.1, 2.0, 1.9, 1.8, 1.7,$ and 1.6 . ^bThe La content is set to 1.

agreement with that of Rietveld refinements. The phenomenon of observed vacancies in these compounds is consistent with RCO_2As_2 ($R = \text{La, Ce, Pr, Nd}$), which were recently reported to have Co vacancies.^{14,15}

The lattice constants and selected atomic distances for LaCo_xAs_2 ($x = 1.98, 1.92, 1.82, 1.70, 1.64,$ and 1.61) derived from structural refinements are schematized in Figure 3. Upon decreasing Co content, a axis slightly lengthens and c axis shortens by about 2%. The As atoms from adjacent layers get closer with As–As distance $d_{\text{As-As}}$ decreasing from 2.907(2) to 2.879(2) Å. The c/a ratio, obtained by the crystallographic data from Supporting Information Table S1, lies in the range from 2.60 to 2.53. These results indicate that LaCo_xAs_2 ($x = 1.98, 1.92, 1.82, 1.70, 1.64,$ and 1.61) are cT phases (which means that the interlayer anion–anion bonding pulls the layers closer and induces a relaxation of the in-plane lattice dimension²⁰) for their $d_{\text{As-As}}$ and c/a are very close to the respective values of the theoretically calculated and pressure-induced cT phase of CaFe_2As_2 .^{21–23} The strong contraction along c axis and expansion in a axis upon increasing vacancy levels can be interpreted from the charge balance point of view. Removal of Co reduces the net cationic charge in the material. This can be balanced by enhancing the As–As bonding ($(\text{As}_2)^{4-}$ has less formal negative charge than $2 \times \text{As}^{3-}$), which contracts c . In a similar manner, introduction of metal vacancy decreases the in-plane metal–metal bonding, which results in an expansion of a axis.

Now, we would address the issue regarding the origin of metal vacancies in ThCr_2Si_2 -type structure through a more comprehensive charge balance point of view. In ThCr_2Si_2 -type

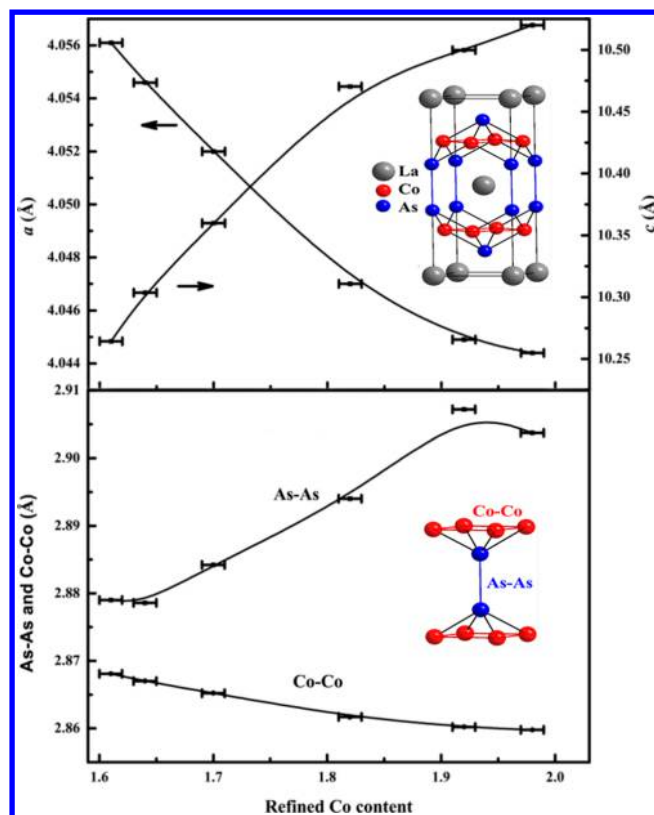


Figure 3. Lattice parameters, As–As and Co–Co distances of LaCo_xAs_2 ($x = 1.98, 1.92, 1.82, 1.70, 1.64,$ and 1.61) as a function of refined Co content.

structure, the transition metal–metalloid layer is negatively charged, whereas the large-sized metal layer positively charged. A charge balance exists between them. In case the balance is tipped, charge compensation always takes into effect by two ways. One is the change in valence of the transition metals and the other is the introduction of vacancies either in the transition metal site or in the large-sized metal site. For example, when K is totally replaced by Sr in KCo_2As_2 , a reduction in Co's valence is expected to maintain the charge balance. Moreover, when Sr is totally replaced by La in SrCo_2As_2 , a further reduction in Co's valence should occur to form LaCo_2As_2 without Co vacancy like in LaCo_2P_2 .^{24–26} But because As–As bonding is present and Co is already in its observed lowest valence, the introduction of Co vacancy is the way to maintain the charge balance. For isostructural $\text{K}_x\text{Fe}_{2-y}\text{Se}_2$, vacancies are present both in K and Fe sites to maintain the charge balance.²⁸ This scenario also applies to compounds beyond the ThCr_2Si_2 -type structure. A typical example is $\text{CeOCu}_{1-x}\text{Se}$ where vacancies reside in Cu site.³¹ This is due to the CeO layer providing more electrons than what CuSe layer can accommodate. The introduction of Cu vacancies is an effective way to maintain the charge balance. So the presence of vacancies is an effective means to keep the charge balance for a compound whose layer is in the state of carrier accommodation limit due to any factors that can induce charge changes. In our case, the As–As bonding is one of these factors responsible for the appearance of Co vacancies.

Figure 4 shows the temperature-dependent magnetic susceptibility of LaCo_xAs_2 ($x = 1.98, 1.92, 1.82, 1.70, 1.64,$ and 1.61). All of them clearly exhibit ferromagnetic ordering. The derivative of magnetic susceptibility shows that T_c varies

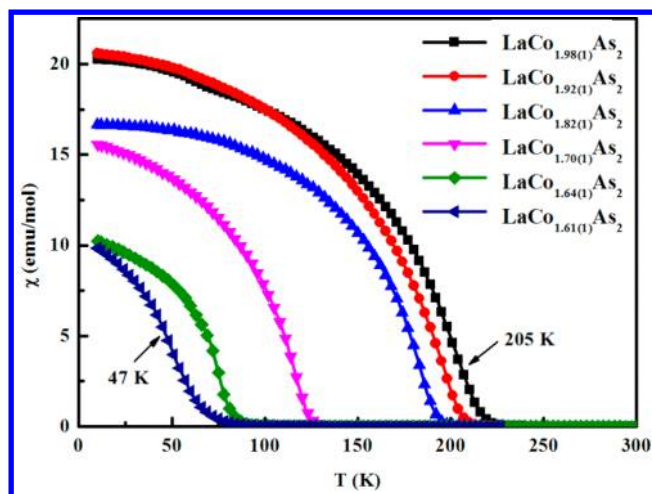


Figure 4. Temperature-dependent magnetic susceptibility of LaCo_xAs_2 ($x = 1.98, 1.92, 1.82, 1.70, 1.64,$ and 1.61) measured at 100 Oe. Arrows indicate the transition temperatures.

from 205 to 47 K with the decreasing Co occupation from 1.98(1) to 1.61(1) (Supporting Information Figure S3). The side phase LaOCoAs with Curie temperature of about 60 K does not interfere with the ferromagnetic transition of LaCo_xAs_2 ,^{27,28} whereas LaAs is paramagnetic. The hysteresis loops at 10 K (Supporting Information Figure S4) indicate that all these compounds are soft ferromagnets with the coercive force ranging from about 2360 to 50 Oe, which is similar to those for $\text{La}_{0.97}\text{Bi}_{0.03}\text{Co}_{1.9}\text{As}_2$ and LaCo_2P_2 .^{15,29} A substantial decrease of the saturation moment from $0.44 \mu_{\text{B}}/\text{Co}$ to $0.24 \mu_{\text{B}}/\text{Co}$ with increasing Co vacancies is observed from the isothermal field dependent magnetization. However, neutron diffraction data collected at 4 K fail to reveal the magnetic order of $\text{LaCo}_{1.92(1)}\text{As}_2$ (Supporting Information Figure S1b). As shown in Table 2, we compare the lattice constants and T_{c} in

Table 2. Comparison of the Lattice Constants and T_{c} between the Reference and This Work

compound	a (Å)	c (Å)	T_{c} (K)
LaCo_2As_2 ^a	4.0536(5)	10.324(2)	86
$\text{LaCo}_{1.70(1)}\text{As}_2$ ^b	4.0520(3)	10.3598(8)	117
$\text{La}_{0.969}\text{Bi}_{0.031}\text{Co}_{1.91}\text{As}_2$ ^a	4.0508(2)	10.470(1)	200
$\text{LaCo}_{1.98(1)}\text{As}_2$ ^b	4.0444(3)	10.5200 (8)	205

^aThe data is from the reference 14. ^bThe data is from this work.

the ref 14 to this work. It is found that the lattice constant and the Curie temperature of LaCo_2As_2 in ref 14 are close to the respective value of our sample $\text{LaCo}_{1.70(1)}\text{As}_2$. So the significantly enhanced T_{c} of $\text{La}_{0.969}\text{Bi}_{0.031}\text{Co}_{1.91}\text{As}_2$ can be interpreted in a new light. It might be closely correlated with the lower Co deficiency.

The temperature-dependent resistivity for LaCo_xAs_2 ($x = 1.61$ and 1.98) exhibits metallic behavior (Supporting Information Figure S5). $\text{LaCo}_{1.61(1)}\text{As}_2$ has a twice larger resistivity than that of $\text{LaCo}_{1.98(1)}\text{As}_2$. For $\text{LaCo}_{1.61(1)}\text{As}_2$, there is a clear quick decrease for resistivity at about 47 K, as shown in the inset of Supporting Information Figure S5, which is near T_{c} of $\text{LaCo}_{1.61(1)}\text{As}_2$. However, the resistivity of $\text{LaCo}_{1.98(1)}\text{As}_2$ shows no anomaly near 200 K. This may be due to the fact that the resistivity contributed from electron-spin dispersion is very small in contrasts to the electron–lattice dispersion.

In order to understand the mechanism of decreased T_{c} and increased resistivity with arising of Co vacancies, we turn to the first-principles calculations. The electronic structure of LaCo_2As_2 exhibits a high peak in the density of states (DOS) at the vicinity of the Fermi level (Supporting Information Figure S6), which accounts for the observed metallic behavior in Supporting Information Figure S5. It also shows that Co atoms contribute the majority DOS near the Fermi level. So the decline of Co content lowers the DOS at the Fermi level, resulting in the increase of resistivity. According to the Stoner criterion,³⁰ an itinerant magnet exhibits ferromagnetism when $I \cdot N(E_{\text{F}}) > 1$, where I is the strength of metal exchange interaction, which can be approximately obtained from the elemental metal,³¹ $N(E_{\text{F}})$ is the DOS at the Fermi level. The calculated value of $I \cdot N(E_{\text{F}})$ is 2.8 for LaCo_2As_2 , which demonstrates the itinerant ferromagnetic ordering in this compound. This result is similar to the isostructural compound LaCo_2P_2 .²⁹ Further calculations of spin-polarized DOS (Supporting Information Figure S7) show that the difference between the spin-up and spin-down DOS channels below the Fermi level is 0.97 states/cell for LaCo_2As_2 . This value declines to 0.74 states/cell for $\text{LaCo}_{1.5}\text{As}_2$. This result means that intralayer Co–Co exchange interaction weakens with increasing Co vacancies, which is consistent with the observed elongated Co–Co distance and lowered T_{c} in Co-deficient LaCo_xAs_2 .

CONCLUSION

In summary, we demonstrate that the nonstoichiometry is an intrinsic feature for LaCo_xAs_2 . The occupancy of Co can be tuned between 1.98(1) and 1.61(1) in LaCo_xAs_2 . We point out that the existence of Co vacancies results from charge balance due to the formation of bond between As–As. Co vacancies lower T_{c} from 205 to 47 K and increase the resistivity by more than 100%. The first-principles calculations indicate that LaCo_2As_2 is an itinerant ferromagnet. The occurrence of Co vacancies lowers the DOS at the Fermi level and weakens the spin polarization, which leads to the increased resistivity and decreased T_{c} , respectively. Knowledge of the key role of Co vacancies in the properties of LaCo_xAs_2 allows the result of ref 14 to be interpreted in a new light. The results address well the importance of in-plane vacancies in the research area of superconductivity and related phenomena in ThCr_2Si_2 -type materials and show the possibility of tuning the magnetism of ThCr_2Si_2 -type structure through transition metal vacancies as well.

ASSOCIATED CONTENT

Supporting Information

Crystallographic data, neutron diffraction patterns and the Rietveld refinements, PXRD patterns and the Rietveld refinements, the derivative magnetic susceptibility and hysteresis loops, resistivity, nonmagnetic DOS and spin-polarized DOS, an X-ray crystallographic file (CIF), and a neutron diffraction crystallographic file (CIF). This material is available free of charge via the Internet at <http://pubs.acs.org>.

AUTHOR INFORMATION

Corresponding Authors

*E-mail: gangwang@iphy.ac.cn.

*E-mail: chenx29@iphy.ac.cn.

Notes

The authors declare no competing financial interest.

ACKNOWLEDGMENTS

S.J.S. thanks Dr. J. Yan from Beihang University for helpful discussions about the neutron diffraction and Q. H. Zhang and X. Chen for assistance in the EDX measurements. This work was partly supported by the National Natural Science Foundation of China (Grant Nos. 51322211 and 90922037), the Strategic Priority Research Program (B) of the Chinese Academy of Sciences (Grant No. XDB07020100), Beijing Nova Program (Grant No. 2011096) and K. C. Wong Education Foundation, Hong Kong.

REFERENCES

- (1) Villars, P.; International, A. *Pearson's Handbook of Crystallographic Data for Intermetallic Phases*, 2nd ed.; ASM International: Novetty, OH, 1991.
- (2) Franz, W.; Griessel, A.; Steglich, F.; Wohlleben, D. *Z. Phys. B: Condens. Matter* **1978**, *31*, 7–17.
- (3) Steglich, F.; Aarts, J.; Bredl, C. D.; Lieke, W.; Meschede, D.; Franz, W.; Schafer, H. *Phys. Rev. Lett.* **1979**, *43*, 1892–1896.
- (4) Fujii, H.; Okamoto, T.; Shigeoka, T.; Iwata, N. *Solid State Commun.* **1985**, *53*, 715–717.
- (5) Jia, S.; Jiramongkolchai, P.; Suchomel, M.; Toby, B.; Checkelsky, J.; Ong, N.; Cava, R. *Nat. Phys.* **2011**, *7*, 207–210.
- (6) Rotter, M.; Tegel, M.; Johrendt, D. *Phys. Rev. Lett.* **2008**, *101*, 107006.
- (7) Guo, J. G.; Jin, S. F.; Wang, G.; Wang, S. C.; Zhu, K. X.; Zhou, T. T.; He, M.; Chen, X. L. *Phys. Rev. B* **2010**, *82*, 180520.
- (8) Ying, T. P.; Chen, X. L.; Wang, G.; Jin, S. F.; Zhou, T. T.; Lai, X. F.; Zhang, H.; Wang, W. Y. *Sci. Rep.* **2012**, *2*, 426.
- (9) Ying, T. P.; Chen, X. L.; Wang, G.; Jin, S. F.; Lai, X. F.; Zhou, T. T.; Zhang, H.; Shen, S. J.; Wang, W. Y. *J. Am. Chem. Soc.* **2013**, *135*, 2951–2954.
- (10) Bobev, S.; Xia, S. Q.; Bauer, E. D.; Ronning, F.; Thompson, J. D.; Sarrao, J. L. *J. Solid State Chem.* **2009**, *182*, 1473–1480.
- (11) Elghadraoui, E. H.; Pivan, J. Y.; Guerin, R.; Pena, O.; Padiou, J.; Sergent, M. *Mater. Res. Bull.* **1988**, *23*, 1345–1354.
- (12) Mewis, A. Z. *Naturforsch., B: J. Chem. Sci.* **1980**, *35*, 141–145.
- (13) Quirinale, D. G.; Anand, V. K.; Kim, M. G.; Pandey, A.; Huq, A.; Stephens, P. W.; Heitmann, T. W.; Kreyssig, A.; McQueeney, R. J.; Johnston, D. C.; Goldman, A. I. *Phys. Rev. B* **2013**, *88*, 174420.
- (14) Thompson, C. M.; Kovnir, K.; Eveland, S.; Herring, M. J.; Shatruk, M. *Chem. Commun.* **2011**, *47*, 5563–5565.
- (15) Thompson, C. M.; Tan, X.; Kovnir, K.; Garlea, V. O.; Gippius, A. A.; Yaroslavtsev, A. A.; Menushenkov, A. P.; Chernikov, R. V.; Büttgen, N.; Krättschmer, W.; Zubavichus, Y. V.; Shatruk, M. *Chem. Mater.* **2014**, *26*, 3825–3837.
- (16) Rodríguez-Carvajal, J. *Phys. B (Amsterdam, Neth.)* **1993**, *192*, 55–69.
- (17) Clark, S. J.; Segall, M. D.; Pickard, C. J.; Hasnip, P. J.; Probert, M. I.; Refson, K.; Payne, M. C. *Z. Kristallogr.* **2005**, *220*, 567–570.
- (18) Perdew, J. P.; Burke, K.; Ernzerhof, M. *Phys. Rev. Lett.* **1996**, *77*, 3865.
- (19) Monkhorst, H. J.; Pack, J. D. *Phys. Rev. B* **1976**, *13*, 5188–5192.
- (20) Jia, S.; Williams, A. J.; Stephens, P. W.; Cava, R. J. *Phys. Rev. B* **2009**, *80*, 165107.
- (21) Goldman, A. I.; Kreyssig, A.; Prokes, K.; Pratt, D. K.; Argyriou, D. N.; Lynn, J. W.; Nandi, S.; Kimber, S. A. J.; Chen, Y.; Lee, Y. B.; Samolyuk, G.; Leao, J. B.; Poulton, S. J.; Bud'ko, S. L.; Ni, N.; Canfield, P. C.; Harmon, B. N.; McQueeney, R. J. *Phys. Rev. B* **2009**, *79*, 024513.
- (22) Kreyssig, A.; Green, M. A.; Lee, Y.; Samolyuk, G. D.; Zajdel, P.; Lynn, J. W.; Bud'ko, S. L.; Torikachvili, M. S.; Ni, N.; Nandi, S.; Leao, J. B.; Poulton, S. J.; Argyriou, D. N.; Harmon, B. N.; McQueeney, R. J.; Canfield, P. C.; Goldman, A. I. *Phys. Rev. B* **2008**, *78*, 184517.
- (23) Yildirim, T. *Phys. Rev. Lett.* **2009**, *102*, 037003.
- (24) Reehuis, M.; Jeitschko, W. *J. Phys. Chem. Solids* **1990**, *51*, 961–968.
- (25) Reehuis, M.; Ritter, C.; Ballou, R.; Jeitschko, W. *J. Magn. Magn. Mater.* **1994**, *138*, 85–93.
- (26) Morsen, E.; Mosel, B. D.; Mullerwarmuth, W.; Reehuis, M.; Jeitschko, W. *J. Phys. Chem. Solids* **1988**, *49*, 785–795.
- (27) Yanagi, H.; Kawamura, R.; Kamiya, T.; Kamihara, Y.; Hirano, M.; Nakamura, T.; Osawa, H.; Hosono, H. *Phys. Rev. B* **2008**, *77*, 224431.
- (28) Sefat, A. S.; Huq, A.; McGuire, M. A.; Jin, R.; Sales, B. C.; Mandrus, D.; Cranswick, L. M.; Stephens, P. W.; Stone, K. H. *Phys. Rev. B* **2008**, *78*, 104505.
- (29) Kovnir, K.; Thompson, C. M.; Zhou, H. D.; Wiebe, C. R.; Shatruk, M. *Chem. Mater.* **2010**, *22*, 1704–1713.
- (30) Stoner, E. C. *Proc. R. Soc. London, Ser. A* **1938**, *165*, 372–414.
- (31) Janak, J. F. *Phys. Rev. B* **1977**, *16*, 255–262.